Wind Energ. Sci. Discuss., doi:10.5194/wes-2016-37, 2016
Manuscript under review for journal Wind Energ. Sci.
Published: 9 December 2016

eawe european academy of wind energy
Open Access WIND ENERGY SCIENCE DISCUSSIONS

Effect of the Foundation Modelling on the Fatigue Lifetime of a Monopile-based Offshore Wind Turbine

Steffen Aasen[1], Ana M. Page[2,3], Kristoffer Skjolden Skau[2,3], Tor Anders Nygaard[1]

[1]Institute for Energy Technology, PO Box 40, 2027 Kjeller, Norway
[2]Norwegian Geotechnical Institute, Sognsveien 72, 0855 Oslo, Norway
[3]Norwegian University of Science and Technology, Department of Civil and Transport Engineering, Høgskoleringen 7A, 7491 Trondheim, Norway

Correspondence to: tor.anders.nygaard@ife.no

Abstract. Several studies have emphasized the importance of modelling foundation response with representative damping and stiffness characteristics in integrated analyses of offshore wind turbines (OWT's). For the monopile foundation, the industry standard for pile-analysis has shown to be inaccurate, and alternative models that simulate foundation behaviour more accurately are needed. As fatigue damage is a critical factor in the design phase, this study investigates how four different soil-foundation models affect the fatigue damage of an OWT with monopile foundation. The study shows how both stiffness and damping properties have a noticeable effect on the fatigue damage, especially for idling cases. At mudline, accumulated fatigue damage varied up to 16% depending on the foundation model used.

Wind Energ. Sci. Discuss., doi:10.5194/wes-2016-37, 2016
Manuscript under review for journal Wind Energ. Sci.
Published: 9 December 2016

eawe european academy of wind energy
Open Access WIND ENERGY SCIENCE DISCUSSIONS

1 Introduction

The last decade there has been a strong tendency to look offshore, to further increase the wind energy potential in Northern Europe. This had led to a total of over 3000 installed OWT's, with a capacity of more than 11GW (December 2015). Large offshore sites with suitable wind conditions are still accessible, and together with strong political intensives this lead to high growth expectations for the industry (EWEA, 2015a). Installation, maintenance and foundation costs tend to increase with distance to shore and water depth, making cost reductions important. So far, improved supply chain integration and large capacity turbines have been the main methods for cost reductions (ORE Catapult, 2015). However, cost reductions also depend on more cost-efficient design. With the support structure contributing up to 20% of the capital cost (EWEA, 2015b), optimizing foundation design has a high potential for cost reductions.

Integrated time domain analysis plays a central role in the design phase of OWT's. Integrated analysis refers to fully coupled analysis of the full OWT system, including rotor, support structure and foundation. The foundation response has significant impact on the dynamic behaviour of the OWT (see Sect. 2.3), which in turn influence the dimensioning of the structure.

For depths up to 30 meters, the monopile is the most common support structure, accounting for approximately 80% of the installations (EWEA, 2015a). This foundation gives long and slender structures sensitive to resonance effects, since wave and wind loads are typically close to the natural frequencies of the structure. Because of this, soil-foundation response can have a high impact on the dynamics of the system and thereby the fatigue damage of the structure. With fatigue damage being a design driver, soil-foundation modelling becomes important in design.

The aim of this paper is to study four different soil-foundation models with respect to their impact on fatigue damage of the OWT structure. Both the conventional method for pile-analysis (p-y curves), and simple linear elastic models, have been compared with a nonlinear elastic model with hysteretic damping. A range of environmental conditions have been simulated to study the soil-foundation models for different loading.

Wind Energ. Sci. Discuss., doi:10.5194/wes-2016-37, 2016
Manuscript under review for journal Wind Energ. Sci.
Published: 9 December 2016

eawe european academy of wind energy
Open Access WIND ENERGY SCIENCE DISCUSSIONS

2 Foundation behaviour

2.1 Observed foundation behaviour

The foundation has to resist the loads transferred from the structure above and remain functional and stable during the lifetime of the OWT. Piles supporting monopile-based OWTs are subjected to large horizontal loads applied with an arm of about 30 – 90 m, which results in large bending moments at the foundation. The applied vertical load is relatively small compared with the horizontal and bending moment loads (Byrne and Houlsby, 2003). Large diameter piles resist these loads by mobilizing lateral resistance in the soil. Due to the interaction between the pile and the soil, the foundation response is influenced by the response of the soil around it. The most important characteristics of soil behaviour with respect to monopiles are:

(1) **Non-linear response**. Soils show non-linear response during loading. In pile foundations, the generation of plastic deformations in the soil around the pile causes plastic displacements and rotations, resulting in a non-linear load-displacement foundation response. This behaviour is illustrated in Figure 1 between points 0 and 1. Several pile tests displaying the non-linear load-displacement response can be found in the literature, see for instance Poulos and Davis (1980), Cox et al. (1974), Reese et al. (1975) for flexible piles or Byrne et al. (2015) for more rigid piles with large diameters typical for monopiles supporting monopile-based OWTs.

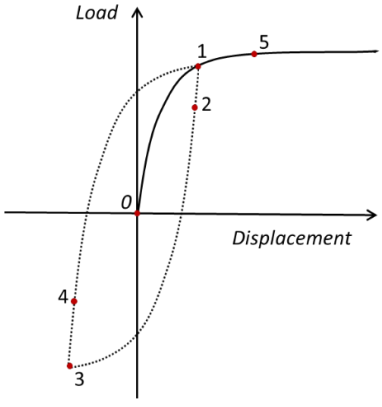

Figure 1: Observed foundation behaviour.

(2) **Different stiffness during loading, unloading and reloading**. Soils exhibit different stiffness during loading, unloading and reloading. When the load acting on the foundation is reversed (points 1 to 2 in Figure 1), the soil around the pile is unloaded. Initially the soil unloading is elastic and the pile response is stiffer than prior to the reversal. As the magnitude of the load reversal increases, more plastic deformations are generated and the stiffness decreases (points 2 to 3). During reloading (points 3 to 5 and back to 1), a similar pattern is observed. This behaviour has been reported in cyclic large- and small-scale pile tests, see for instance Little and Briaud (1988), Roesen et al. (2013) or in centrifuge tests, e.g. Klinkvort et al. (2010), Bienen et al. (2011) or Kirkwood (2015).

Wind Energ. Sci. Discuss., doi:10.5194/wes-2016-37, 2016
Manuscript under review for journal Wind Energ. Sci.
Published: 9 December 2016

(3) **Damping**. Two different types of damping are present in foundation problems: radiation damping, where the energy is dissipated through geometric spreading of the waves propagating through the soil, and hysteretic damping, where energy is dissipated due to plastic deformations. Radiation damping depends on the loading frequency, and it is negligible for frequencies below 1 Hz (Andersen, 2010). Hysteretic soil damping depends on the strain level in the soil and is affected by the loading history. For monopiles supporting OWT's, radiation damping can be neglected, and the main damping contribution comes from hysteretic damping. The hysteretic nature of the foundation damping has been noted in free vibration tests (Hanssen et al., 2016), where the foundation damping decreased with decreasing displacement amplitude. The hysteretic loss of energy at foundation level is illustrated in Figure 1 in the enclosed area defined by points 1-2-3-4-1. Hysteretic load displacement loops can also be observed in cyclic large- and small-scale pile tests and in centrifuge tests (Klinkvort et al., 2010, Roesen et al., 2013).

Full-scale measurements of monopile-based OWTs also confirm the non-linear hysteretic foundation response. Kallehave et al. (2015) observed that the measured natural frequency of monopile-based OWTs decreased with increasing wind speeds, and related it to the increasing displacement levels. The same conclusion was reached by Damgaard et al. (2013) when analysing the reduction in natural frequency with increasing acceleration levels.

For OWT's in operation (Damgaard et al., 2013, Shirzadeh et al., 2013, Tarp-Johansen et al., 2009, Versteijlen et al., 2011) found foundation damping between 0.25-1.5 % of critical damping depending load level and soil profile.

2.2 Current foundation modelling

The industry standard for representing the pile response in integrated analyses of monopile-based OWTs is based in the so-called *p-y* curve approach. In the *p-y* curve methodology, the pile is modelled as a beam and the soil is represented as a series of discrete, uncoupled, non-linear elastic springs at nodal points along the pile. The springs relate the local lateral resistance, *p*, to the local lateral displacement of the pile, *y*, and are function of the depth below mudline. The DNV standard (Det Norske Veritas, 2014) recommends the use of API *p-y* curves (API, 2011) for the estimation of the lateral pile capacity in ULS analyses. However, the *p-y* curves were developed for long and slender jacket piles with large length-to-diameter ratios, significantly different to typical monopile geometries. Several studies have shown the limitations of the *p-y* curve approach (Doherty and Gavin, 2011, Lesny, 2010, Jeanjean, 2009, Hearn and Edgers, 2010), and alternatives to the API formulation have been proposed, such as *p-y* curves extracted from FE analysis of the soil-foundation system. Despite these curves being able to capture the pile stiffness more accurately, the same extracted *p-y* curve is often used in the simulation tools for loading, unloading and reloading, which means that they neglect effects such as permanent deformations and soil damping. In this regard, Det Norske Veritas (2014) require soil-damping to be considered in the design phase, but no recommended practice for estimating soil damping is suggested.

Wind Energ. Sci. Discuss., doi:10.5194/wes-2016-37, 2016
Manuscript under review for journal Wind Energ. Sci.
Published: 9 December 2016

eawe european academy of wind energy
Open Access WIND ENERGY SCIENCE DISCUSSIONS

2.3 Numerical studies investigating effects of soil stiffness and damping

Some studies have been carried out to investigate the impact of soil stiffness and damping on the structural response of monopile-based OWTs. Schafhirt et al. (2016) examined the effect of variations in the soil stiffness on the equivalent damage loads for a monopile in sand by using *p-y* curves with different stiffness. The study suggest that a reduction of 50% in the soil stiffness lead to an increase of 7% in the equivalent damage loads at mudline. Damgaard et al. (2015) studied the impact of a change in soil stiffness and damping on the fatigue loads, where the foundation was represented by a lumped-parameter model. They found that a 50% reduction of the soil's Young modulus, increased the fatigue damage equivalent moment at mudline by approximately 12%; and a 50% reduction of the soil damping properties increased the fatigue damage equivalent moment by 25%. Carswell et al. (2015) studied the effect of soil damping for an OWT with monopile foundation subjected to extreme storm loading. The hysteretic damping was computed using a nonlinear elastic two dimensional finite element model, and included in the foundation model by a viscous rotational damper at mudline. From stochastic time history analysis they found that maximum and standard deviation of mudline moment was reduced by 7-9% due to soil damping. These contributions highlight the impact of the soil stiffness and damping on the fatigue loads. However, each of these studies uses different soil profiles and modelling approaches to represent the foundation stiffness and damping, which makes a comparison between the different foundation models and damping contributions difficult. On this regard, Jung et al. (2015) carried out a comparison between three foundation models with focus on the foundation stiffness. In the study, the foundation response was represented by a stiffness matrix at mudline, distributed *p-y* elements and a finite element (FE) model of the soil volume. Foundation damping was neglected. It was found that the bending moments calculated by using the *p-y* approach and the FE approach were very similar.

In this study, the aim is to evaluate the impact of foundation stiffness and damping through the foundation modelling approach on the fatigue damage of a monopile-based OWT in a lifetime perspective. For that purpose, four different foundation models have been calibrated for the same soil profile, and a series of simulations representative for the OWT lifetime have been performed. The results in terms of accumulated fatigue damage are presented and discussed.

Wind Energ. Sci. Discuss., doi:10.5194/wes-2016-37, 2016
Manuscript under review for journal Wind Energ. Sci.
Published: 9 December 2016

3 Modelling of OWT and foundation

3.1 3DFloat

The simulation software 3DFloat has been used for modal analysis and time domain simulations. 3DFloat is an aero-servo-hydro-elastic Finite-Element-Method code, developed by IFE and NMBU. This means that hydrodynamic loads, aerodynamic loads and the control system are considered, when calculating the elastic response of the system. 3DFloat has been verified and validated in the IEA OC3, OC4 and OC5 projects, wave tank tests and by participation in commercial projects. For more details, see Nygaard et al. (2016).

Structural elements are modelled by Euler-Bernoulli beams with 12 degrees of freedom. Loads from gravity, buoyancy, waves, current and wind are applied as distributed external loads on the structure. For elements in water, a combination of wave kinematics and force models are used. Forces from waves and currents on slender beams, are calculated by the relative form of Morison's equation. In this study, combinations of airy wave components according to the JONSWAP spectrum were used to simulate irregular sea states.

Aerodynamic forces on the rotor blades are calculated with Blade Element Momentum Theory, with enhancement for dynamic inflow and yaw errors.

Currently new soil-foundation models are implemented in 3DFloat as part of the research project REDWIN (www.ngi.no/eng/Projects/REDWIN). Previously, crude springs and dampers have modelled soil resistance. As part of this study, a nonlinear model with hysteretic damping has been implemented in the code, referred to as Model 3.

3.2 Soil-foundation models

Four approaches have been used to model the pile-foundation response. Model 1-3 give the full loading response from the soil-pile system at a single node connected to the superstructure. Model 4 refer to the conventional distributed p-y element approach. Of the four models, Model 2 and Model 3 account for soil damping.

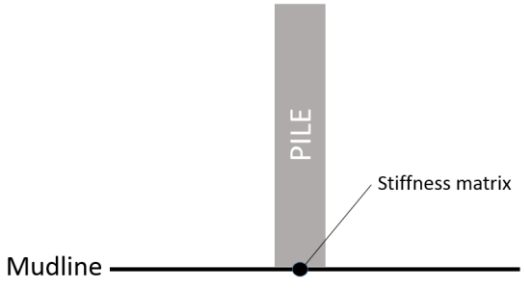

Figure 2: 2D representation of Model 1.

Wind Energ. Sci. Discuss., doi:10.5194/wes-2016-37, 2016
Manuscript under review for journal Wind Energ. Sci.
Published: 9 December 2016

3.2.1 Model 1

This model applies a linear elastic stiffness matrix at the mudline to represent the pile-foundation response. By this approach, the model neglects nonlinear effects and damping. A 2D representation of the model is given in Figure 2. The stiffness coefficients should reflect the load level considered to best represent modal properties of the system.

3.2.2 Model 2

Model 2 applies a stiffness matrix like in Model 1, but with additional rotational dampers to model soil damping. A 2D representation of the system is given in Figure 3. Rotational dampers are chosen, as moment typically dominates mudline loading for OWT monopile (Carswell et al., 2015). The rotational dampers are implemented at the mudline node. The moment responses from the rotational dashpots are given by:

$$M_c = c \cdot \omega \tag{1}$$

, where *c [Nm s/rad]* is a damping coefficient, and *ω [rad/s]* is the angular frequency. This makes damping a function of frequency. As explained in Sect. 2.1, hysteretic damping dominates the damping from the foundation. As this is a function of load level and not frequency, the damping coefficient should be calibrated for a given load level and load frequency. Knowing the hysteretic energy loss due to soil damping per load cycle, a rotational dashpot for a single degree of freedom system can be found by:

$$c = \frac{E_h(M)}{2\theta^2\pi^2\omega} \tag{2}$$

, where $E_h(M)$[J] is the hysteretic energy loss per load cycle, θ[rad] is the angular displacement amplitude, and ω[rad/s] is the angular frequency of the system.

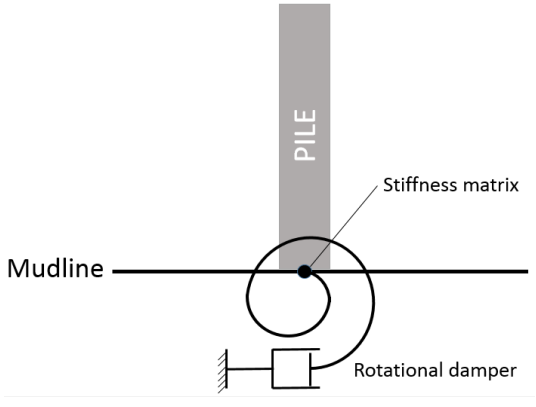

Figure 3: 2D representation of Model 2.

Wind Energ. Sci. Discuss., doi:10.5194/wes-2016-37, 2016
Manuscript under review for journal Wind Energ. Sci.
Published: 9 December 2016

eawe european academy of wind energy
Open Access WIND ENERGY SCIENCE DISCUSSIONS

3.2.3 Model 3

Model 3 is a non-linear 1D rotational model, where the stiffness depends on the load level. A 2D representation of the model is given in Figure 4.

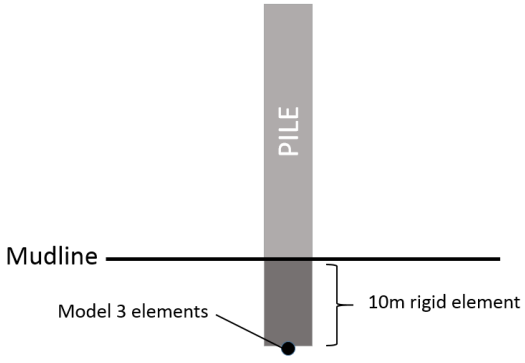

Figure 4: 2D representation of Model 3.

The model follows Masing's rule and produce hysteretic damping and different stiffness during loading, unloading and reloading. The model is formulated following the approach suggested by Iwan (1967) where several linear elastic-perfectly plastic springs are coupled in parallel. The nonlinear load-displacement behaviour of the foundation load is the sum of all spring loads. Each of the springs has different stiffness and yield load, but forced to have the same deformation. After a spring has yielded in compression it will become linear elastic after reversal and remain elastic until it reaches the same value in tension. The stiffness will change when the load in a single spring reach the yield load of that spring, making the overall load-displacement behaviour piecewise-linear and behave according to a kinematic hardening rule. The load-displacement curve can be represented sufficiently smooth by using a high number of coupled springs. Figure 5 illustrates how the behaviour of the individual springs are combined to a total nonlinear hysteretic response.

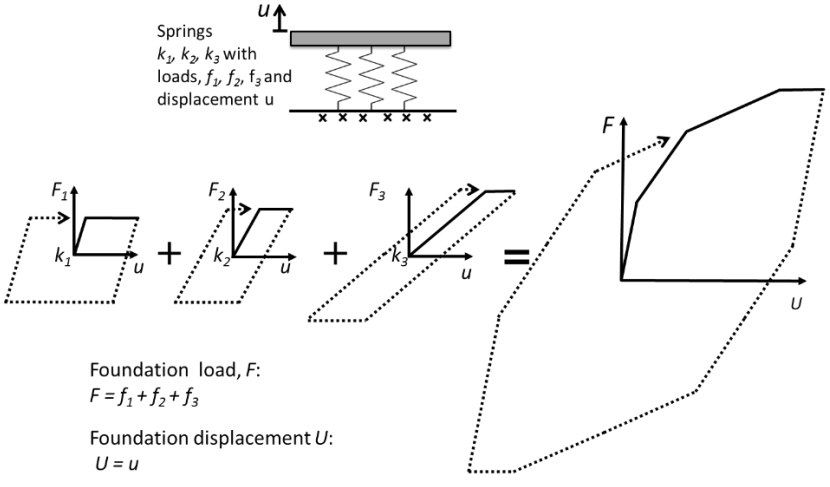

Figure 5: A combination of spring-slip elements can model a system with hysteretic behaviour.

Wind Energ. Sci. Discuss., doi:10.5194/wes-2016-37, 2016
Manuscript under review for journal Wind Energ. Sci.
Published: 9 December 2016

The model is applied to the rotational DOF, with the load-displacement behaviour according to the moment-rotation behaviour. To reflect both the rotation and horizontal displacement at mudline, the model is applied 9.5 meters below the mudline. A rigid beam connect the model to the flexible tower at mudline.

3.2.4 Model 4

Model 4 includes an extension of the monopile below mudline, and refer to the p-y-element approach where nonlinear elastic springs are distributed along the pile and provide the soil resistance at different depths. The model does not include any damping. A 2D representation of the model is given in Figure 6. To represent the varying soil conditions at different depths, each spring has different soil-reaction displacement characteristics. A typical shape of a p-y curve for sand is given in Figure 7.

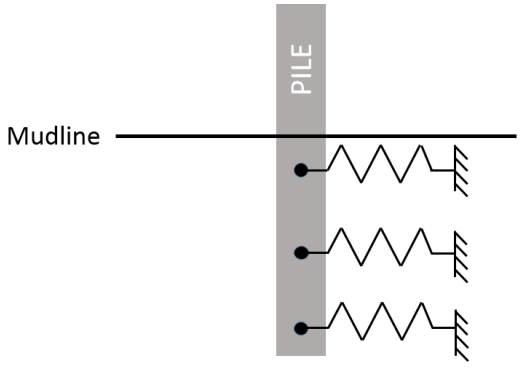

Figure 6: 2D representation of Model 4.

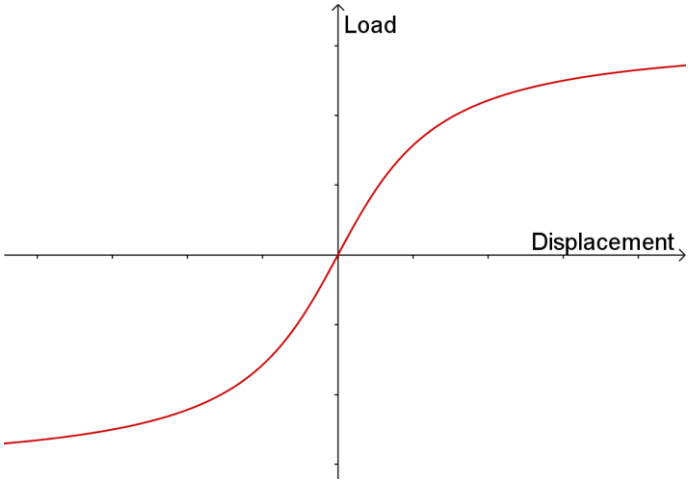

Figure 7: Typical shape of p-y curves for sand.

Wind Energ. Sci. Discuss., doi:10.5194/wes-2016-37, 2016
Manuscript under review for journal Wind Energ. Sci.
Published: 9 December 2016

eawe european academy of wind energy
Open Access WIND ENERGY SCIENCE DISCUSSIONS

4 Case Study

4.1 Structural properties of OWT

The NREL 5MW Wind turbine, with monopile foundation according to OC3 Phase II (Jonkman and Musial, 2010), has been used in this study. The structure is developed to support concept studies for offshore wind turbines, and is a utility-scale multi-megawatt wind turbine, with a three bladed upwind variable-speed variable-blade-pitch-to-feather-controlled turbine (Jonkman et al., 2009). An overview of the structural dimensions is given in Figure 8. For details about the structure, the reader is referred to (Jonkman et al., 2009). The transition piece has not been modelled and the pile properties are extended up to the tower in the 3DFloat model.

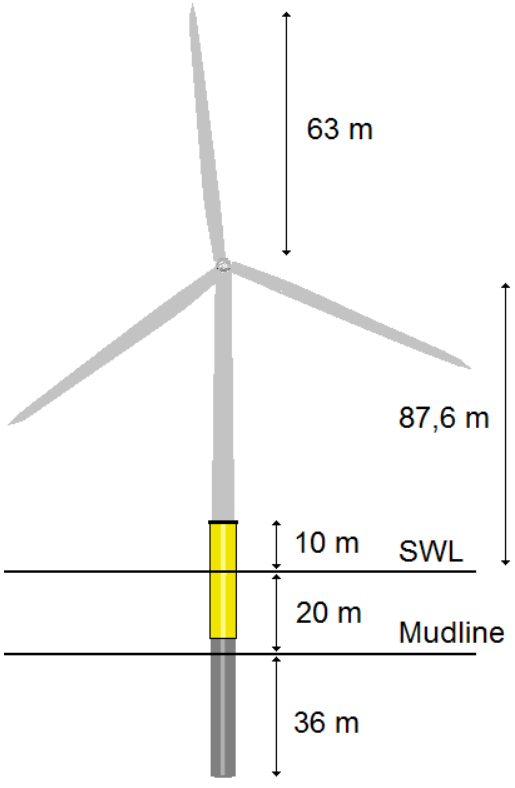

Figure 8: Dimensions of the NREL 5MW wind turbine, with monopile foundation.

4.2 Soil profile

The soil profile has been taken from OC3, Phase II (Jonkman and Musial, 2010). It is a three layered profile, with effective unity weigh, γ', of 10 [kN/m^3] and varying angle of friction, ϕ' [°], representing a medium dense sand. The stiffness of the p-y curves increases proportionally with depth according to the effective stress increase from the weight of soil. A representation of the soil layers and pile dimensions is given in Figure 9.

Wind Energ. Sci. Discuss., doi:10.5194/wes-2016-37, 2016
Manuscript under review for journal Wind Energ. Sci.
Published: 9 December 2016

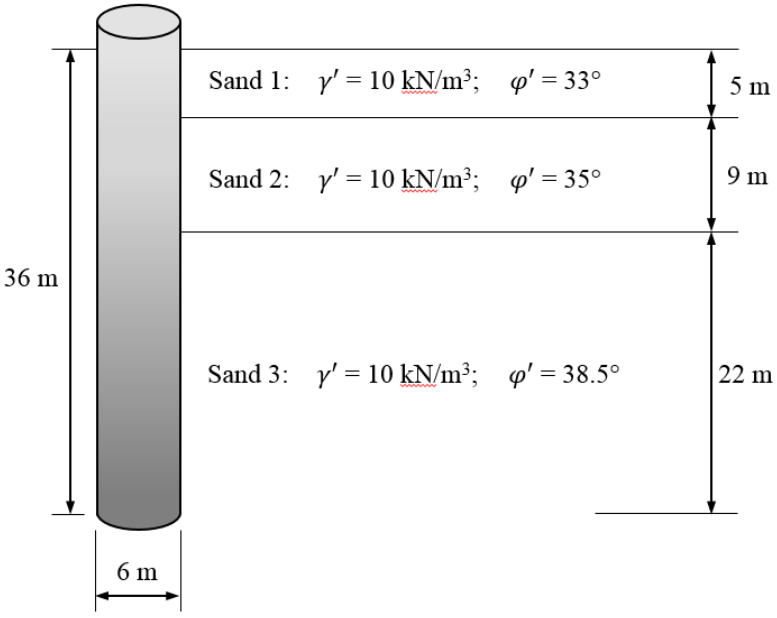

Figure 9: Soil profile and pile dimensions.

4.3 Environmental conditions

Environmental conditions, representing a possible site for monopile installation in the North Sea have been used in the analyses. A lumped scatter diagram of wind and waves, generated for fatigue damage calculations, was taken from the Upwind Design Basis for a shallow water site with 25m depth (Fischer et al., 2010). The lumped scatter diagram is generated to limit the number of load cases, while giving equivalent fatigue damage to real site wind and wave conditions.

Waves and wind are unidirectional, normal to the rotor plane, as the focus of this study has been dynamics in the fore-aft plane. A presentation of wind and wave data is given in Table 1.

For generation of turbulence, the Mann 64bit turbulence generator, provided by the HAWC2 project is used (www.hawc2.dk). Wind speed is given at the hub height, and a power law, with wind shear exponent of 0.14, gives the wind profile.

Superposition of airy wave components given by the JONSWAP spectrum with a gamma factor of 2.87 is used to generate the irregular wave kinematics.

Wind Energ. Sci. Discuss., doi:10.5194/wes-2016-37, 2016
Manuscript under review for journal Wind Energ. Sci.
Published: 9 December 2016

Table 1: Environmental conditions.

Load case	*U_wind [m/s]*	*Ti [%]*	*Hs [m]*	*Tp [s]*	*Pro_occ*
1	2	29.2	1.07	6.03	0.0671
2	4	20.4	1.10	5.88	0.08911
3	6	17.5	1.18	5.76	0.14048
4	8	16.0	1.31	5.67	0.13923
5	10	15.2	1.48	5.74	0.14654
6	12	14.6	1.70	5.88	0.14272
7	14	14.2	1.91	6.07	0.08381
8	16	13.9	2.19	6.37	0.08316
9	18	13.6	2.47	6.71	0.04186
10	20	13.4	2.76	6.99	0.03480
11	22	13.3	3.09	7.40	0.01535
12	24	13.1	3.42	7.80	0.00974
13	26	12.0	3.76	8.14	0.00510
14	28	11.9	4.17	8.49	0.00202
15	30	11.8	4.46	8.86	0.00096

U_wind	Wind speed at hub height
Ti	Turbulence intensity
H	Significant wave height
Tp	Spectral peak period
Pro_occ	Probability of occurrence

4.4 Calibration of soil-foundation models

4.4.1 Calibration of Model 1

Parameters for the foundation stiffness matrix has been according to the coupled-springs model of OC3 Phase II (Jonkman and Musial, 2010). Simple soil-foundation models were calibrated for the project by Passon (2006). As stiffness coefficients were produced for a 2D system, the stiffness matrix has simply been extended to a 3D system, by using the same stiffness coefficients along both horizontal axes. By this approach, coupling effects between the two horizontal axes are neglected. However, since mainly in plane loads are consider, the simplification is considered to be acceptable.

Passon (2006) estimated the stiffness coefficients by calculating the secant pile stiffness at mudline at a given load level with the geotechnical code LPILE. In these analyses, the pile was modelled as a beam and the pile-soil interface and soil response were modelled as uncoupled lateral p-y springs. The secant stiffness was calculated for 1.5 times the ULS loads. This should be considered as a low stiffness estimate. The stiffness coefficients are given in Eq. (3)

Wind Energ. Sci. Discuss., doi:10.5194/wes-2016-37, 2016
Manuscript under review for journal Wind Energ. Sci.
Published: 9 December 2016

$$\begin{bmatrix} k_{xx} & 0 & 0 & 0 & k_{x\beta} & 0 \\ 0 & k_{yy} & 0 & k_{y\alpha} & 0 & 0 \\ 0 & 0 & 0 & 0 & 0 & 0 \\ 0 & k_{\alpha y} & 0 & k_{\alpha\alpha} & 0 & 0 \\ k_{\beta x} & 0 & 0 & 0 & k_{\beta\beta} & 0 \\ 0 & 0 & 0 & 0 & 0 & 0 \end{bmatrix} \quad \begin{aligned} k_{xx} = k_{yy} &= 2.57481 \cdot 10^{9} && [N/m] \\ k_{\alpha\alpha} = k_{\beta\beta} &= 2.62912 \cdot 10^{11} && [Nm/rad] \\ k_{x\beta} = k_{\beta x} &= -2.25325 \cdot 10^{10} && [N/rad], [N] \\ k_{y\alpha} = k_{\alpha y} &= 2.25325 \cdot 10^{10} && [N/rad], [N] \end{aligned} \tag{3}$$

, where x and y are displacements in the horizontal plane, and α and β are rotations around the corresponding axe. Wind and waves are aligned with the x-axis for all load cases in this paper. Figure 10 gives a conceptual representation of the moment rotation curve at mudline for the different models. As seen, the foundation stiffness for Model 1 is independent of load level.

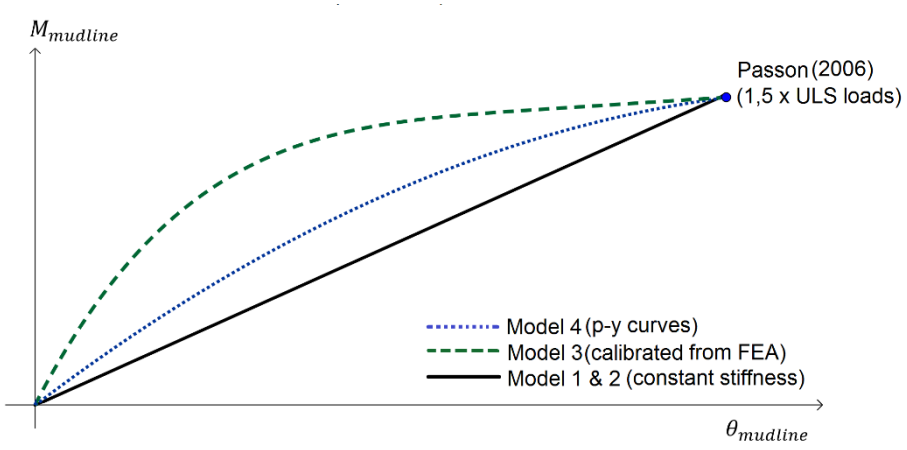

Figure 10: Stiffness as a function of load level for the different models. The figure is conceptual, and differences between the models are exaggerated.

4.4.2 Calibration of Model 2

Model 2 uses the same stiffness matrix as Model 1, giving it the same stiffness profile as Model 1 (Figure 10). In addition, viscous rotational dampers have been included at the mudline, around both horizontal axes, to account for soil damping. The viscous dampers have been calibrated to give a foundation damping factor of approximately 1% near rated wind speed conditions (load case 6). This is considered reasonable and in line with studies from literature (Shirzadeh et al., 2013, Carswell et al., 2014). The foundation damping ratio of 1 % expresses the hysteretic energy loss in the soil as a percentage of the total elastic strain energy of the soil. If the soil damping factor is expressed as the hysteretic energy loss in the soil as a percentage of the total strain energy of the complete OWT structure, the 1% damping value would decrease to 0.3%.

To see how soil damping affects fatigue damage, two other calibrations for the damping coefficients has been chosen, which gives foundation damping factors of 0,5% and 1,5% near rated conditions (load case 6). The calibrations for the rotational dampers is given in Table 2. The damping coefficients have been held constant for all load cases, as opposed to Model 3, where damping is load-dependent.

Wind Energ. Sci. Discuss., doi:10.5194/wes-2016-37, 2016
Manuscript under review for journal Wind Energ. Sci.
Published: 9 December 2016

Table 2: Model 2 damping parameters

	$c_{\alpha\alpha}, c_{\beta\beta}$ *[Nm-s/rad]*	*Foundation damping Factor (D)**	*Foundation damping Ratio (ξ_{fdn})**
Model 2a	4.67e8	~0.5%	~0.15%
Model 2b	9.34e8	~1.0%	~0.3%
Model 2c	1.40e9	~1.5%	~0.45%

**Calculations are done for a natural frequency of 0,25 Hz*

4.4.3 Calibration of Model 3

A finite element analysis of the soil-pile system was performed to obtain moment-rotation and horizontal load-displacement curves at the mudline. The analysis was performed with the geotechnical finite element software PLAXIS 3D, with a horizontal load H applied to the pile with an arm of 40 m above the mudline. Figure 11 illustrates the mesh and the dimensions of the finite element model. Due to symmetry of the geometry and the loading, only half of the problem was modelled.

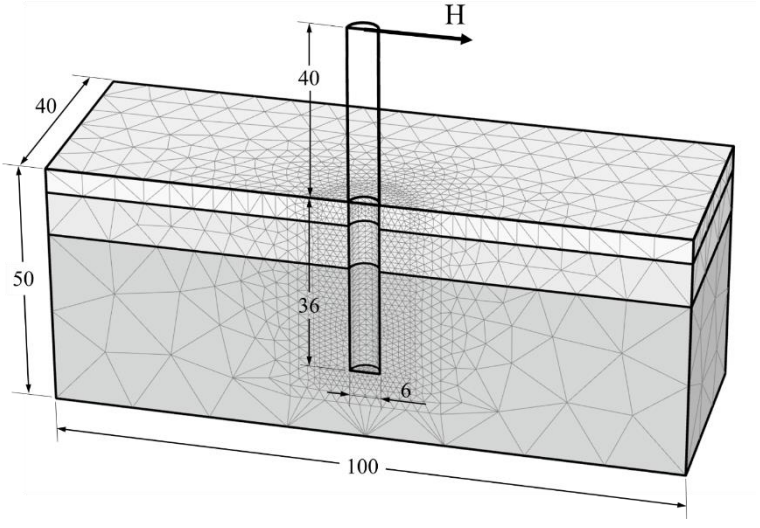

Figure 11: Mesh and dimensions of the finite-element model.

The Hardening Soil Small Strain constitutive model (Benz, 2007, Brinkgreve et al., 2013) was used to represent the sand behaviour. This constitutive model captures the very small strain soil stiffness and its non-linear dependency on the strain amplitude, and it is suitable for analyses of geotechnical structures in sand subjected to small-amplitude loading. Due to lack of soil test data, the parameters of the model were correlated from the relative density (RD) of the three sand layers based on the relations proposed by Brinkgreve et al. (2010). The relative densities of the sand layers were derived from the friction angle (ϕ') documented in Passon (2006) through the expression:

$$\phi' = 28 + RD/8 \quad (4)$$

Wind Energ. Sci. Discuss., doi:10.5194/wes-2016-37, 2016
Manuscript under review for journal Wind Energ. Sci.
Published: 9 December 2016

Model 3 was calibrated by fitting the computed bending moment – rotation curve at mudline from finite element analyses, as illustrated in Figure 12. The results from Passon (2006), used in the calibration of Models 1 and 2, are included as a reference. In addition, the comparison between the computed bending moment – horizontal displacement curve (Figure 13) was used to determine the point of application of Model 3. The best fit was obtained when Model 3 was located 9.5 m below mudline. Figure 10 shows the stiffness of Model 3, compared with the other models. Seen relative to the other models, it gives a stiffer behaviour for low load levels, and for higher load levels, the behaviour is softer.

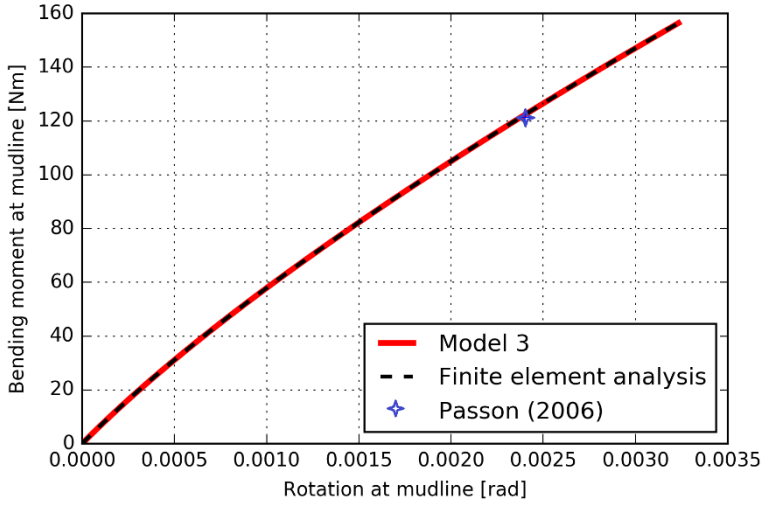

Figure 12: Computed moment – rotation curve at mudline from finite element analyses and from the calibrated Model 3. The representative moment and rotation at mudline used in the calibration from Passon (2006) are included as a reference.

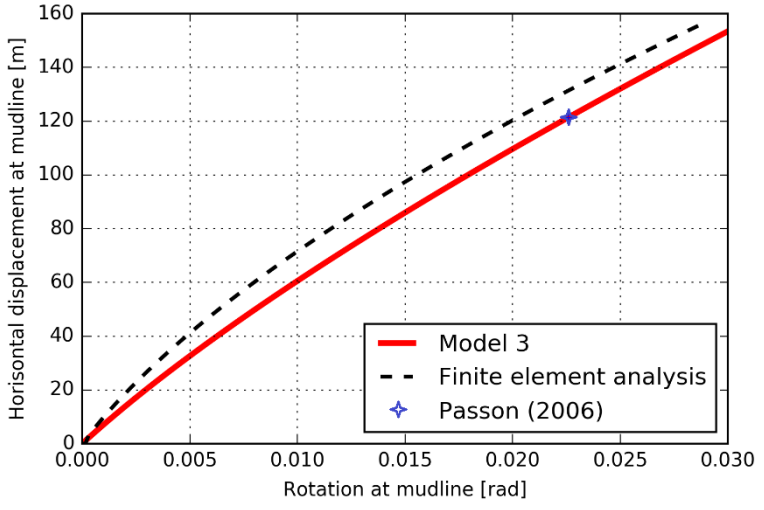

Figure 13: Computed moment – horizontal displacement curve at mudline from finite element analyses and from the calibrated Model 3. The representative moment and rotation at mudline used in the calibration from Passon (2006) are included as a reference.

Wind Energ. Sci. Discuss., doi:10.5194/wes-2016-37, 2016
Manuscript under review for journal Wind Energ. Sci.
Published: 9 December 2016

eawe european academy of wind energy
Open Access WIND ENERGY SCIENCE DISCUSSIONS

4.4.4 Calibration of Model 4

The p-y curves generated by Passon (2006) for OC3 Phase II, which follow the API sand model, have been used in this study. The reader is referred to Passon (2006) for more details. In the load region relevant for this study, the p-y curves show little nonlinearity (Figure 10).

4.5 Fatigue damage calculations

Fatigue damage has been calculated by the S-N curve approach, using Palmer-Miner's rule according to DNV standards (Det Norske Veritas, 2010). S-N curves gives the number of cycles before failure, for given stress ranges, $\Delta\sigma$. With variable stress ranges, linear cumulative damage is assumed, according to the Palmer-Miner rule. The total damage at a given location is given by:

$$D = \sum_{i=1}^{k} \frac{n_i}{N_i} \tag{5}$$

, where all stress cycles are collected in k number of stress blocks. D is the accumulated fatigue damage (failure when D=1), n_i is the number of stress cycles in block i, and N_i is the number for cycles before failure for stress block i.

S-N curves for steel in air are used, even though some of the positions for fatigue damage calculation are exposed to seawater. This will give misleading absolute values for positions exposed to water, but as relative values are of main interest in this study, this has not been considered. S-N curve F3 for air, from table 7-14 in the DNV standard DNV-OS-J101 (DNV, 2014) are used in fatigue calculations, and are according to:

$$\log_{10} N = \log_{10} a - m \log_{10}\left(\Delta\sigma \left(\frac{t}{t_{ref}}\right)^{k}\right) \tag{6}$$

, where N are the number of stress cycles before failure at stress range $\Delta\sigma$, m is the negative slope of the logN-logS curve, $\log_{10} a$ is the intercept of the logN axis, t_{ref} is a reference thickness, t is the thickness through which the potential fatigue crack will grow, and k is a thickness exponent. The S-N curve has different parameters, depending on the number of stress cycles. Parameter values used in this thesis are given in Table 3.

The duration of each load case is 1800 seconds. Results have been extrapolated to find the accumulated fatigue damage per year. When extrapolating data, some stress cycles will enter the high cycle region ($N > 10^7$), where damage is higher for a given stress range. As this has not been accounted for, absolute values should be evaluated accordingly. This will not influence relative values, as this affects calculations for all the soil models.

Wind Energ. Sci. Discuss., doi:10.5194/wes-2016-37, 2016
Manuscript under review for journal Wind Energ. Sci.
Published: 9 December 2016

eawe european academy of wind energy
Open Access WIND ENERGY SCIENCE DISCUSSIONS

Table 3: S-N curve parameters

	$N<10^7$	$N>10^7$
$\log_{10} a$	11.546	14.576
m	3.0	5.0
k	0.25	0.25
t_{ref}	25mm	25mm

Wind Energ. Sci. Discuss., doi:10.5194/wes-2016-37, 2016
Manuscript under review for journal Wind Energ. Sci.
Published: 9 December 2016

eawe european academy of wind energy
Open Access WIND ENERGY SCIENCE DISCUSSIONS

5 Analysis

5.1 Model characteristics from free vibration tests

A free vibration test was performed to identify the basic characteristics of each the foundation models in terms of stiffness and damping. A forced displacement of 0.2 m at the tower top was applied and released before the tower was allowed to vibrate freely. The results are presented in Figure 14 and Figure 15.

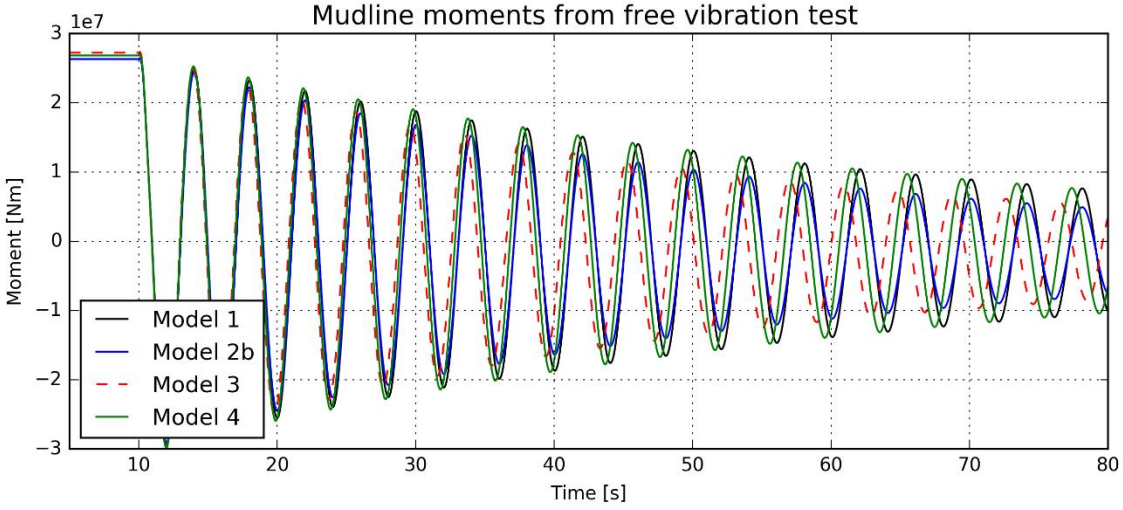

Figure 14: Free vibration test with a tower top displacement of 0.2 m.

Model 1 and 2 give the same 1st natural fore-aft frequency for the structure, as the mudline stiffness is the same. Model 3 and 4 shows stiffer behaviour. The damping contribution from the different models is quantified by the global damping ratio, which is given as percentage of critical damping. It include soil-, structural-, aerodynamic- and hydrodynamic damping. The disturbances in the first eight cycles are due energy exchange with higher order modes. As damping sources other than soil damping is the same for all models, the differences are due the damping properties of the soil-foundation models. It can be seen how soil damping from Model 3 is reduced with decreasing load amplitude, but for the other models, damping remains constant (except from the first cycles with disturbances from other modes). The soil damping ratio for Model 2 is constantly 0.3%, and for Model 3 it varies between 0.05% - 0.3%. The load amplitudes in the free vibration test is representative for load case 6 – 15.

Wind Energ. Sci. Discuss., doi:10.5194/wes-2016-37, 2016
Manuscript under review for journal Wind Energ. Sci.
Published: 9 December 2016

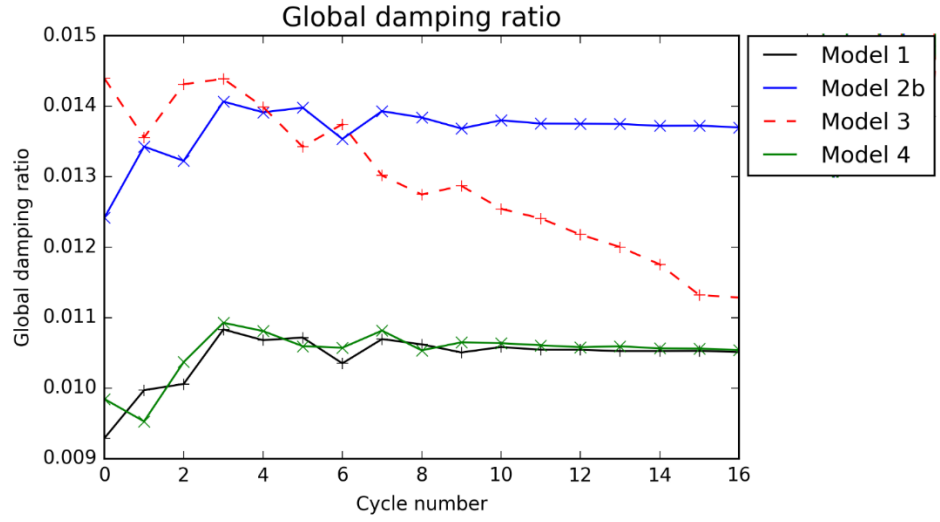

Figure 15: Global damping ratio for the foundation models.

5.2 Foundation model impact on fatigue damage

The total accumulated fatigue damage per year is plotted in Figure 16. It can be seen that Model 1 gives the highest fatigue damage, and Model 3 the lowest, with a reduction of roughly 16% relative to Model 1. The reduction is a consequence of a favourable increase in both stiffness and damping in Model 3 compared to Model 1. By comparing the Models 1, 2a, b and c it can be seen that soil damping magnitude has a significant effect on the fatigue damage at the mudline. A 50% increase in soil-damping magnitude, leads to 4% reduction in accumulated fatigue damage.

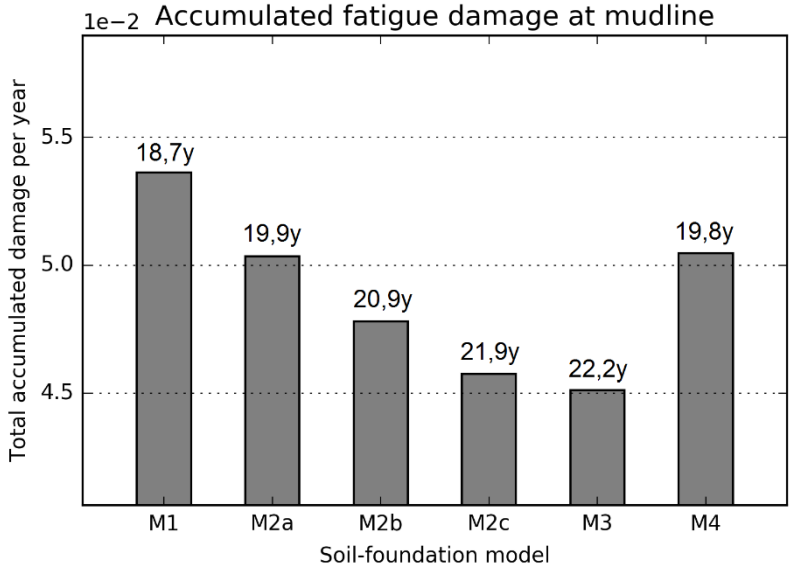

Figure 16: Accumulated fatigue damage at mudline.

Wind Energ. Sci. Discuss., doi:10.5194/wes-2016-37, 2016
Manuscript under review for journal Wind Energ. Sci.
Published: 9 December 2016

Comparing the p-y curve approach (Model 4), with the linear elastic model (Model 1), it can be seen how the nonlinear foundation stiffness influence fatigue damage. The softer Model 1 takes the natural frequency of the structure closer to wave frequencies than the stiffer Model 4, thereby increasing resonance effects. In addition to the total accumulated fatigue damage per year, the expected fatigue life time is given in years (y) at the top of each column.

Figure 17 presents the relative accumulated fatigue damage by load case. Results are normalized relative to the highest value. Each load case is also probability weighed, according to Table 1. It can be seen how the foundation models have the highest impact on idling cases (LC 1 & 13-15). This has mainly two reasons: 1) LC 1 and LC 13-15 are load cases where the rotor is idling, and as a consequence aerodynamic damping is highly reduced. Thus the soil damping has a higher share of the total damping of the system. 2) Load amplitudes are higher. This leads to more damping from Model 3, while damping from Model 2a-c is unchanged. It can be seen how Model 3 gives fatigue damage at the level of Model 2b in operational cases, but lower fatigue damage in the idling cases where the damping in Model 3 is higher.

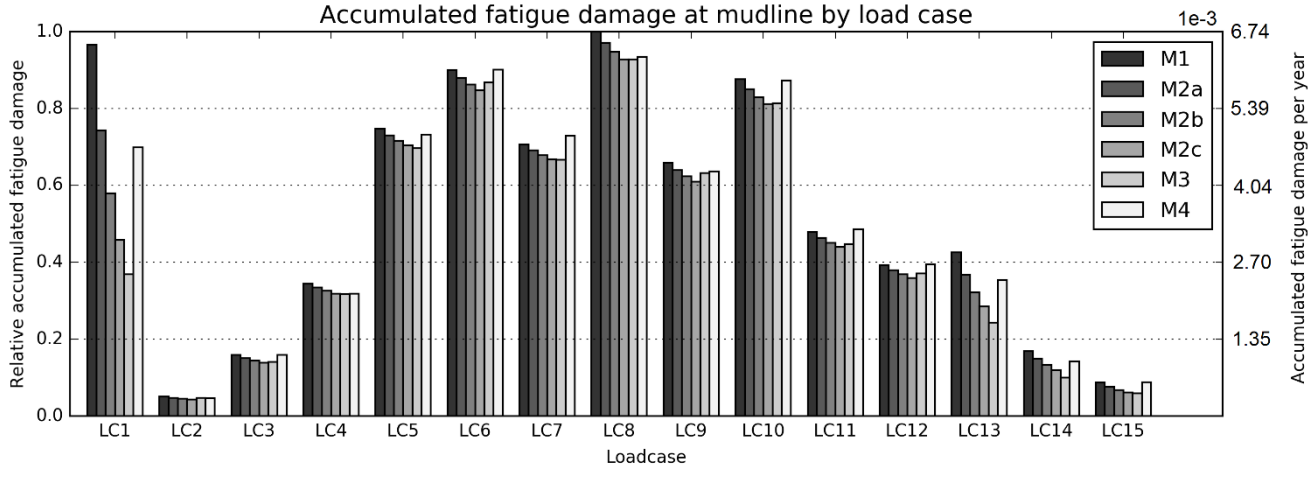

Figure 17: Accumulated fatigue damage at mudline arranged after load case.

Load case 1 has a high impact on the total fatigue damage. This might seem counterintuitive, as wind and wave loads are relatively low. However, with little aerodynamic damping, the tower is free to oscillate at its first natural frequency, leading to high load amplitudes at the mudline, even though absolute values are small. Together with a high probability of occurrence, this gives a significant contribution to the total fatigue damage.

Fatigue damage calculations at the tower root (10m above still water line) are given in Figure 18 and Figure 19. Absolute values are highly reduced, but relative effect of the soil-foundation model, shows to be even higher at this location. The trends are similar to what was observed at the mudline.

Calculations was also done for the tower top and blade root. As the soil-foundation model had very little impact here (<1% change in fatigue damage), the results are not included in this paper. On these locations rotor dynamics dominate the loading, which are not considerably influenced by the soil-foundation response.

Wind Energ. Sci. Discuss., doi:10.5194/wes-2016-37, 2016
Manuscript under review for journal Wind Energ. Sci.
Published: 9 December 2016

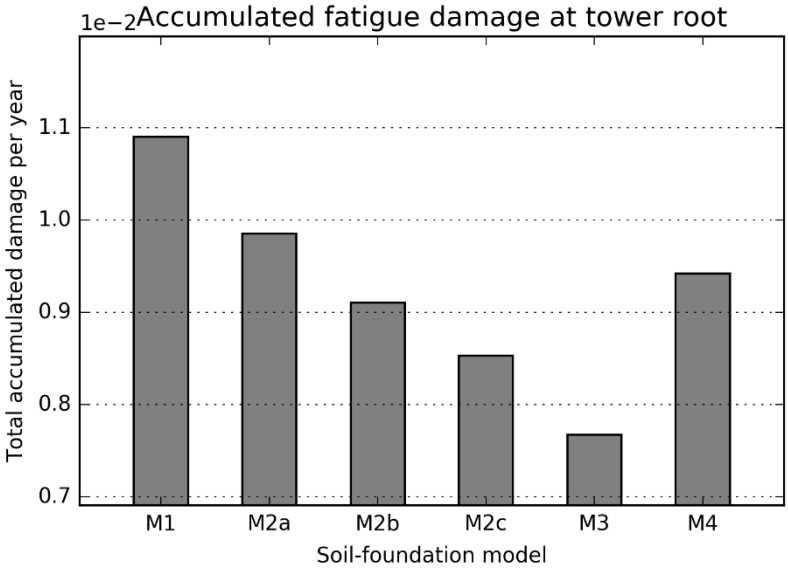

Figure 18: Accumulated fatigue damage at tower root

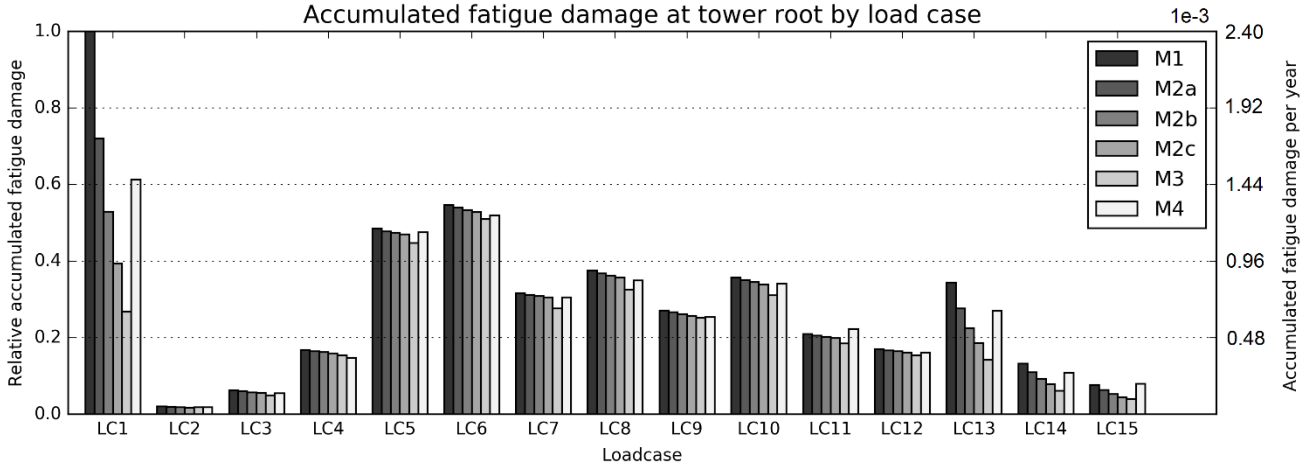

Figure 19: Accumulated fatigue damage at tower root arranged after load case.

5

Wind Energ. Sci. Discuss., doi:10.5194/wes-2016-37, 2016
Manuscript under review for journal Wind Energ. Sci.
Published: 9 December 2016

6 Conclusions and further work

Comparing different soil-foundation models show how both stiffness and damping properties influence the fatigue damage of an OWT with monopile foundation. The results clearly show that choosing an appropriate conceptual foundation model can have significant positive effects and that determination of parameters for whatever chosen model is equally important.

The nonlinear rotational model (Model 3), which reflect foundation behaviour most realistically was shown to improve the fatigue life time expectancy. Comparing it with the current industry standard (Model 4), the accumulated fatigue damage at mudline was reduced by 11%, and with respect to the linear elastic model (Model 1), the reduction was 16%. The nonlinear rotational model (Model 3) has positive effect on fatigue life as a consequence of both its damping and stiffness properties. Figure 10 illustrates how Model 3 is stiffer when the loading amplitude is small, which is true for the majority of operational time. This brings the natural frequency of the system away from wave frequencies, resulting in less resonance effects. In addition to this, the model gives damping as a function of load amplitude, giving more damping at high loads levels (Figure 15). Both effects reduce the load amplitude. As fatigue damage grows exponentially with load amplitude, this has positive effect on fatigue life.

The linear elastic model with damping (Model 2) has also shown how damping by itself has noticeable effect on fatigue damage. Compared to Model 1 (linear-elastic) with similar stiffness, fatigue damage was reduced by 11% (Model 2a), with a foundation damping ratio of 0.3%.

This study, along with other studies of bottom-fixed offshore wind turbines, has brought the attention to idling cases, where the absence of aerodynamic damping and high probability of occurrence gives both a high contribution to the total fatigue damage, and a high sensitivity to the foundation model. The study has used a lumped wind/wave diagram, with both wind and waves acting in the same direction. This should be revisited in the continuation of this work, as cases with offsets between wind and wave directions could lead to relatively high excitation from the waves, and low aerodynamic damping in the direction of the waves. The details of the foundation model could here become even more important.

Wind Energ. Sci. Discuss., doi:10.5194/wes-2016-37, 2016
Manuscript under review for journal Wind Energ. Sci.
Published: 9 December 2016

7 Author contributions

	Aasen	Page	Skjolden-Skau	Nygaard
On the research idea and outline of the paper				
Research idea		x	x	
Structure of the research		x	x	x
Outline of the paper		x	x	x
Literature review	x	x		
On the implementation of foundation models				
Implementation of Models 1, 2 and 4 in 3DFloat				x
Implementation of Model 3			x	
Implementation of the interface between 3DFloat and Model 3				x
On the calibration of foundation models				
Calibration of Models 1 and 2	x			
Calibration of Model 3		x	x	
Calibration of Model 4		x	x	
On the simulations				
Building the simulation models in 3DFloat	x			x
Carrying out the simulations	x			
Extracting results from the simulations	x			
On analysing and discussing the results				
Analysing the simulation results	x			
Discussion of the simulation results	x	x	x	x

5

Wind Energ. Sci. Discuss., doi:10.5194/wes-2016-37, 2016
Manuscript under review for journal Wind Energ. Sci.
Published: 9 December 2016

eawe european academy of wind energy
Open Access WIND ENERGY SCIENCE DISCUSSIONS

8 Competing interests

The authors declare that they have no conflict of interest.

Wind Energ. Sci. Discuss., doi:10.5194/wes-2016-37, 2016
Manuscript under review for journal Wind Energ. Sci.
Published: 9 December 2016

eawe european academy of wind energy
Open Access WIND ENERGY SCIENCE DISCUSSIONS

9 Acknowledgements

The financial support by the Norwegian Research Council through the project Reducing Cost of Offshore Wind by Integrated Structural and Geotechnical Design (REDWIN), Grant No. 243984, is gratefully acknowledged. The authors also want to acknowledge the support from Hans Petter Jostad, NGI (in the discussion of the initial research idea), Jörgen Johansson, NGI (in the definition of the structure of the research and in the calibration of Model 2), Jacobus Bernardus De Vaal, IFE (in setting up the 3Dfloat input) and Gudmund Reidar Eiksund, NTNU (in reviewing the final document).

Wind Energ. Sci. Discuss., doi:10.5194/wes-2016-37, 2016
Manuscript under review for journal Wind Energ. Sci.
Published: 9 December 2016

eawe european academy of wind energy
Open Access WIND ENERGY SCIENCE DISCUSSIONS

10 References

ANDERSEN, L. 2010. Assessment of lumped-parameter models for rigid footings. *Computers & Structures,* 88**,** 1333-1347.

API 2011. Recommended Practice for Planning, Designing and Constructing Fixed Offshore Platforms - Working Stress Design. Twenty-first edition ed.: American Petroleum Institute.

BENZ, T. 2007. *Small-strain stiffness of soils and its numerical consequences*, Univ. Stuttgart, Inst. f. Geotechnik.

BIENEN, B., DÜHRKOP, J., GRABE, J., RANDOLPH, M. F. & WHITE, D. J. 2011. Response of piles with wings to monotonic and cyclic lateral loading in sand. *Journal of Geotechnical and Geoenvironmental Engineering,* 138**,** 364-375.

BRINKGREVE, R., ENGIN, E. & ENGIN, H. 2010. Validation of empirical formulas to derive model parameters for sands. *Numerical methods in geotechnical engineering (eds T. Benz and S. Nordal)***,** 137-142.

BRINKGREVE, R., ENGIN, E. & SWOLFS, W. 2013. PLAXIS 3D 2013 User manual. Plaxis bv.

BYRNE, B. & HOULSBY, G. 2003. Foundations for offshore wind turbines. *Philosophical Transactions of the Royal Society of London A: Mathematical, Physical and Engineering Sciences,* 361**,** 2909-2930.

BYRNE, B., MCADAM, R., BURD, H., HOULSBY, G., MARTIN, C., GAVIN, K., DOHERTY, P., IGOE, D., ZDRAVKOVIĆ, L. & TABORDA, D. Field testing of large diameter piles under lateral loading for offshore wind applications. Proceedings of the 16th European Conference on Soil Mechanics and Geotechnical Engineering, Edinburgh, UK, 2015.

CARSWELL, W., JOHANSSON, J., LØVHOLT, F., ARWADE, S. R. & DEGROOT, D. J. Dynamic Mudline Damping for Offshore Wind Turbine Monopiles. ASME 2014 33rd International Conference on Ocean, Offshore and Arctic Engineering, 2014. American Society of Mechanical Engineers, V09AT09A025-V09AT09A025.

CARSWELL, W., JOHANSSON, J., LØVHOLT, F., ARWADE, S. R., DEGROOT, D. J. & MYERS, A. T. 2015. Foundation damping and the dynamics of offshore wind turbine monopiles. *Renewable Energy,* 80**,** 724-736.

CATAPULT, O. 2015. Cost Reduction Monitoring Framework Summary Report to OWPB.

COX, W. R., REESE, L. C. & GRUBBS, B. R. Field testing of laterally loaded piles in sand. Offshore Technology Conference, 1974. Offshore Technology Conference.

DAMGAARD, M., ANDERSEN, L. V. & IBSEN, L. B. 2015. Dynamic response sensitivity of an offshore wind turbine for varying subsoil conditions. *Ocean Engineering,* 101**,** 227-234.

DAMGAARD, M., IBSEN, L. B., ANDERSEN, L. V. & ANDERSEN, J. 2013. Cross-wind modal properties of offshore wind turbines identified by full scale testing. *Journal of Wind Engineering and Industrial Aerodynamics,* 116**,** 94-108.

DET NORSKE VERITAS 2010. Fatigue design of offshore steel structures. *No. DNV-RP-C203*.

DET NORSKE VERITAS 2014. Design of offshore wind turbine structures. Det Norske Veritas.

DOHERTY, P. & GAVIN, K. 2011. Laterally loaded monopile design for offshore wind farms. *Proceedings of the Institution of Civil Engineers,* 165**,** 7-17.

EWEA 2015a. The European offshore wind industry - key trends and statistics 2015. EWEA.

EWEA 2015b. Aiming High - Rewarding Ambition in Wind Energy. European Wind Energy Association.

FISCHER, T., DE VRIES, W. & SCHMIDT, B. 2010. UpWind Design Basis (WP4: Offshore foundations and support structures). Upwind.

HANSSEN, S. B., EIKSUND, G. & NORDAL, S. 2016. Impact vibration test of monopile foundation model in dry sand. *International Journal of Physical Modelling in Geotechnics,* 16**,** 65-82.

HEARN, E. & EDGERS, L. Finite element analysis of an offshore wind turbine monopile. GeoFlorida 2010: Advances in Analysis, Modeling & Design, 2010. ASCE, 1857-1865.

IWAN, W. D. 1967. On a class of models for the yielding behavior of continuous and composite systems. *Journal of Applied Mechanics,* 34**,** 612-617.

JEANJEAN, P. Re-assessment of py curves for soft clays from centrifuge testing and finite element modeling. Offshore Technology Conference, 2009. Offshore Technology Conference.

JONKMAN, J., BUTTERFIELD, S., MUSIAL, W. & SCOTT, G. 2009. Definition of a 5-MW reference wind turbine for offshore system development. *National Renewable Energy Laboratory, Golden, CO, Technical Report No. NREL/TP-500-38060*.

Wind Energ. Sci. Discuss., doi:10.5194/wes-2016-37, 2016
Manuscript under review for journal Wind Energ. Sci.
Published: 9 December 2016

JONKMAN, J. & MUSIAL, W. 2010. Offshore code comparison collaboration (OC3) for IEA task 23 offshore wind technology and deployment.

JUNG, S., KIM, S.-R., PATIL, A. & HUNG, L. C. 2015. Effect of monopile foundation modeling on the structural response of a 5-MW offshore wind turbine tower. *Ocean Engineering*, 109**,** 479-488.

KALLEHAVE, D., THILSTED, C. L. & TROYA, A. 2015. Observed variations of monopile foundation stiffness. *In:* MEYER, V., ed. Frontiers in Offshore Geotechnics III, 2015 Oslo. Taylor & Francis Group, 557-562.

KIRKWOOD, P. B. 2015. *Cyclic lateral loading of monopile foundations in sand.* Doctor of Philosophy, University of Cambridge.

KLINKVORT, R. T., LETH, C. T. & HEDEDAL, O. Centrifuge modelling of a laterally cyclic loaded pile. International Conference on Physical Modelling in Geotechnics, 2010. 959-964.

LESNY, K. 2010. *Foundations for Offshore Wind Turbines: Tools for Planning and Desing*, VGE-Verlag.

LITTLE, R. L. & BRIAUD, J.-L. 1988. Full scale cyclic lateral load tests on six single piles in sand. DTIC Document.

NYGAARD, T. A., DE VAAL, J., PIERELLA, F., OGGIANO, L. & STENBRO, R. 2016. Development, Verification and Validation of 3DFloat; Aero-Servo-Hydro-Elastic Computations of Offshore Structures. *EERA DeepWind'2016*, Energy Procedia, Vol 94, September 2016, Pages 425-433.

PASSON, P. 2006. Memorandum: derivation and description of the soil-pile-interaction models. *IEA-Annex XXIIII Subtask*, 2.

POULOS, H. G. & DAVIS, E. H. 1980. *Pile foundation analysis and design*.

REESE, L. C., COX, W. R. & KOOP, F. D. Field testing and analysis of laterally loaded piles om stiff clay. Offshore Technology Conference, 1975. Offshore Technology Conference.

ROESEN, H. R., IBSEN, L. B., HANSEN, M., WOLF, T. K. & RASMUSSEN, K. L. Laboratory testing of cyclic laterally loaded pile in cohesionless soil. The Twenty-third International Offshore and Polar Engineering Conference, 2013. International Society of Offshore and Polar Engineers.

SCHAFHIRT, S., PAGE, A. M., EIKSUND, G. & MUSKULUS, M. 2016. Influence of Soil Parameters on Fatigue Lifetime for Offshore Wind Turbines with Monopile Support Structure. *EERA DeepWind'2016*, Energy Procedia, Vol 94, September 2016, Pages 347-356.

SHIRZADEH, R., DEVRIENDT, C., BIDAKHVIDI, M. A. & GUILLAUME, P. 2013. Experimental and computational damping estimation of an offshore wind turbine on a monopile foundation. *Journal of Wind Engineering and Industrial Aerodynamics*, 120**,** 96-106.

TARP-JOHANSEN, N. J., ANDERSEN, L., CHRISTENSEN, E. D., MØRCH, C. & FRANDSEN, S. 2009. Comparing sources of damping of cross-wind motion.

VERSTEIJLEN, W., METRIKINE, A., HOVING, J., SMIDT, E. & DE VRIES, W. Estimation of the vibration decrement of an offshore wind turbine support structure caused by its interaction with soil. Proceedings of the EWEA Offshore 2011 Conference, Amsterdam, The Netherlands, 29 November-1 December 2011, 2011. European Wind Energy Association.